Published in final edited form as:
Neuroimage. 2013 December ; 83: . doi:10.1016/j.neuroimage.2013.06.045.

Heterogeneous Impact of Motion on Fundamental Patterns of Developmental Changes in Functional Connectivity During Youth

Theodore D. Satterthwaite, M.D., M.A.[a,*], **Daniel H. Wolf, M.D., Ph.D.**[a,*], **Kosha Ruparel, M.S.E.**[a], **Guray Erus, Ph.D.**[b], **Mark A. Elliott, Ph.D.**[b], **Simon B. Eickhoff, M.D., Ph.D.**[c,d,e], **Efstathios D. Gennatas, M.B.B.S**[a], **Chad Jackson, M.S.E.**[a], **Karthik Prabhakaran, M.S.**[a], **Alex Smith, Ph.D.**[b], **Hakon Hakonarson, M.D., Ph.D.**[f], **Ragini Verma, Ph.D.**[b], **Christos Davatzikos, Ph.D.**[b], **Raquel E. Gur, M.D., Ph.D.**[a,b], and **Ruben C. Gur, Ph.D.**[a,b,g]

[a]Department of Psychiatry, University of Pennsylvania, Philadelphia PA 19104, USA

[b]Department of Radiology, University of Pennsylvania, Philadelphia PA 19104, USA

[c]Department of Psychiatry and Psychotherapy, RWTH Aachen University, Aachen, Germany

[d]Institute of Clinical Neuroscience and Medical Psychology, Heinrich Heine University, Düsseldorf, Germany

[e]Institute for Neuroscience and Medicine (INM-1), Research Center Jülich, Germany

[f]Center for Applied Genomics, Children's Hospital of Philadelphia, Philadelphia PA 19104, USA

[g]Philadelphia Veterans Administration Medical Center, Philadelphia PA 19104, USA

Abstract

Several independent studies have demonstrated that small amounts of in-scanner motion systematically bias estimates of resting-state functional connectivity. This confound is of particular importance for studies of neurodevelopment in youth because motion is strongly related to subject age during this period. Critically, the effects of motion on connectivity mimic major findings in neurodevelopmental research, specifically an age-related strengthening of distant connections and weakening of short-range connections. Here, in a sample of 780 subjects ages 8–22, we re-evaluate patterns of change in functional connectivity during adolescent development after rigorously controlling for the confounding influences of motion at both the subject and group level. We find that motion artifact inflates both overall estimates of age-related change as well as specific distance-related changes in connectivity. When motion is more fully accounted for, the prevalence of age-related change as well as the strength of distance-related effects is substantially reduced. However, age-related changes remain highly significant. In contrast, motion artifact tends to obscure age-related changes in connectivity associated with segregation of functional brain modules; improved preprocessing techniques allow greater sensitivity to detect increased within-module connectivity occurring with development. Finally, we show that subject's age can still be

Please address correspondence to: Theodore Satterthwaite, M.D., M.A, Brain Behavior Laboratory, 10th Floor, Gates Building, Hospital of the University of Pennsylvania, Philadelphia, PA 19104, sattertt@upenn.edu.
*Drs. Satterthwaite and Wolf contributed equally to this manuscript.

DISCLOSURES: Authors report no disclosures.

accurately estimated from the multivariate pattern of functional connectivity even while controlling for motion. Taken together, these results indicate that while motion artifact has a marked and heterogeneous impact on estimates of connectivity change during adolescence, functional connectivity remains a valuable phenotype for the study of neurodevelopment.

Keywords

motion artifact; fMRI; connectivity; development; adolescence; network; connectome; resting-state

INTRODUCTION

Within the growing field of brain connectomics, substantial attention has focused on how brain connectivity develops during youth (Supekar et al., 2009; Power et al., 2010; Fair et al., 2007). This focus is motivated by the marked changes in behavior, emotion, and cognition that occur during this period (Somerville and Casey, 2010; Luna, 2009; Casey et al., 2008). Furthermore, major neuropsychiatric illnesses often begin in youth, underscoring the need to understand how connectivity changes relate to both normal development as well as vulnerability to disease (Paus et al., 2008; Insel, 2009).

Many studies of brain development in youth have examined resting-state functional connectivity MRI (rsfc-MRI), which is based on correlations of the blood-oxygen level dependent (BOLD) signal in different brain regions while subjects are not performing a task (Biswal et al., 1995; Fox and Raichle, 2007). In particular, three prominent rsfc-MRI findings have shaped our understanding of how the brain develops during youth. First, long-range connections tend to strengthen with age, whereas shorter-range connections tend to weaken with age (Supekar et al., 2009; Fair et al., 2007; Dosenbach et al., 2010). Second, large-scale functional brain networks tend to become more segregated from each other with age. As part of this process of segregation, within-network connectivity strengthens while between-network connectivity weakens (Supekar et al., 2009; Fair et al., 2007; Fair et al., 2008; Dosenbach et al., 2010; Anderson et al., 2011). For example, Fair et al. (2007) found that the default mode network (DMN) and the executive system network became more segregated from each other with development, with greater within-network (e.g., DMN-DMN) connectivity and less between-network (e.g., executive-DMN) network connectivity. Third, Dosenbach et al. (2010) demonstrated that this complex pattern of connectivity change can be summarized using multivariate analyses to derive a functional maturation index that is highly correlated with subject age (Dosenbach et al., 2010; see also Wang et al., 2012).

However, since the time that these studies were published, it has been demonstrated in several independent datasets that even small amounts of in-scanner subject motion can systematically bias estimates of resting-state functional connectivity (Van Dijk et al., 2011; Power et al., 2012; Satterthwaite et al., 2012). Notably, the reported effects of motion are exactly opposite of several reported age effects. Specifically, motion is related to a decrease in long-range connectivity and increase in short-range connectivity, which is the inverse of the aforementioned distance-dependent change in connectivity previously observed during development. As motion is inversely correlated with age (i.e., younger children move more), this raises the possibility that motion artifact has driven previously published developmental findings. It is therefore necessary to re-evaluate previous findings in developmental connectivity while accounting for motion artifact more rigorously.

Accordingly, in the present study we revisit age-related changes in functional connectivity in a very large sample of children, adolescents, and young adults (n=780) studied as part of the Philadelphia Neurodevelopmental Cohort (Gur et al., 2012). Specifically, we re-evaluate:

1. The overall predominance of age-related connectivity change. If motion were to inflate age-related connectivity changes, we would expect that strategies that account for motion would diminish apparent age-related changes in connectivity.
2. Distance-dependence of age-related connectivity changes. Similarly, we expect that better control of motion artifact would reduce the apparent distance-dependence of age-related changes, as motion artifact increases short-range connectivity and diminishes long-range connectivity.
3. Network segregation with age. It is unknown how motion impacts the previously-reported strengthening of within-module connections and weakening of between-module connections, which may represent functional segregation of large-scale brain networks. Here we investigate the impact of motion artifact on the evolution of these effects.
4. Prediction of subject age using multivariate patterns of connectivity. Finally, we re-evaluate the degree to which complex patterns of brain connectivity can yield an accurate prediction of subject age even after accounting for motion.

For each analysis, we compare apparent effects of age when data is processed using standard methods and following processing using an improved confound regression model that substantially mitigates the impact of motion on the subject-level timeseries (Satterthwaite et al., 2013; see also Power et al., 2012; Power et al., 2012b; Carp 2012; and Yan et al., 2013 for further discussion). However, even improved methods do not completely eliminate motion artifact. Accordingly, we additionally control for motion in group-level analyses by including it as a confounding covariate. As described below, results reveal that previously reported patterns of neurodevelopmental changes in functional connectivity are differentially impacted by motion artifact. While distance-related age effects diminish, changes related to network segregation are actually enhanced when controlling for motion. Finally, while the accuracy of age prediction using multivariate patterns of connectivity is somewhat diminished by controlling for motion, it nonetheless remains relatively robust. Overall, we demonstrate that while motion may have biased certain aspects of previous findings, functional connectivity remains a valuable phenotype for studying neurodevelopmental change during youth.

METHODS

Participants

The present report is based on data acquired as part of by the Philadelphia Neurodevelopmental Cohort, a collaboration between the Center for Applied Genomics at Children's Hospital of Philadelphia (CHOP) and the Brain Behavior Laboratory at the University of Pennsylvania (Penn). Study procedures were approved by the Institutional Review Boards of both Penn and CHOP. The target population-based sample is of 10,000 youths who presented to the CHOP network for a pediatric visit and volunteered to participate in genomic studies of complex pediatric disorders (Gur et al., 2012). A subsample of 1,445 subjects, stratified by age and sex, were randomly selected for neuroimaging. Of these, 1,275 had resting-state data acquired; 495 subjects were excluded for poor data quality or a history that suggested potential abnormalities of brain development. Specifically, subjects were excluded due to a history of medical problems that might affect brain function, a history of inpatient psychiatric hospitalization, or current use of psychotropic medication. Additionally, subjects were excluded if scan mean relative

displacement (MRD, see below) exceeded 0.2mm, if there were >20 volumes with relative displacement >0.25mm, or if gross between-run motion resulted in incomplete brain coverage. These exclusion criteria resulted in a final sample of 780 subjects aged 8–22 years (mean age 15.6 years, S.D. 3.3 years; 333 males; see Table 1).

Image acquisition

All data were acquired on the same scanner (Siemens Tim Trio 3 Tesla, Erlangen, Germany; 32 channel head coil) using the same imaging sequences. Blood oxygen level dependent (BOLD) fMRI was acquired using a whole-brain, single-shot, multi-slice, gradient-echo (GE) echoplanar (EPI) sequence with the following parameters: 124 volumes, TR 3000 ms, TE 32 ms, flip angle 90°, FOV 192×192 mm, matrix 64X64, slice thickness/gap 3mm/0mm, effective voxel resolution 3.0×3.0×3.0mm. Prior to functional timeseries acquisition, a magnetization-prepared, rapid acquisition gradient-echo (MPRAGE) T1-weighted image was acquired to aid spatial normalization to standard atlas space, using the following parameters: TR 1810 ms, TE 3.51 ms, FOV 180×240 mm, matrix 256×192, 160 slices, TI 1100 ms, flip angle 9 degrees, effective voxel resolution of 0.9 × 0.9 × 1mm. Additionally, a B0 field map was acquired for application of distortion correction procedures, using a double-echo gradient recall echo (GRE) sequence: TR 1000 ms, TE1 2.69 ms, TE2 5.27 ms, 44 slices, slice thickness 4mm, FOV=240mm, effective voxel resolution of 3.8×3.8×4mm. Prior to scanning, in order to acclimate subjects to the MRI environment and to help subjects learn to remain still during the actual scanning session, a mock scanning session was conducted using a decommissioned MRI scanner and head coil. Mock scanning was accompanied by acoustic recordings of the noise produced by gradient coils for each scanning pulse sequence. During these sessions, feedback regarding head movement was provided using the MoTrack motion tracking system (Psychology Software Tools, Inc, Sharpsburg, PA). Motion feedback was only given during the mock scanning session. In order to further minimize motion, prior to data acquisition subjects' heads were stabilized in the head coil using one foam pad over each ear and a third over the top of the head. During the resting-state scan, a fixation cross was displayed as images were acquired. Subjects were instructed to stay awake, keep their eyes open, fixate on the displayed crosshair, and remain still.

Motion metric

As previously (Satterthwaite et al. 2012; Satterthwaite et al., 2013) we evaluated in-scanner head motion using the re-alignment parameters estimated using FSL's MCFLIRT routine (Jenkinson et al., 2002). This estimation derives a motion transformation matrix for each time point. Each transform is described by six motion parameters consisting of three translations and three rotations (Jenkinson et al., 2002). This six parameter timeseries can be condensed to a single vector representing the root mean squared volume-to-volume displacement of all brain voxels (Jenkinson et al., 2002). This one-dimensional motion timeseries can be calculated to measure the RMS displacement relative to a single reference volume (absolute displacement), or relative to the preceding volume (relative displacement). As prior (Satterthwaite et al. 2012; Satterthwaite et al., 2013), we focus on relative RMS displacement. In order to provide a summary measure of motion for each subject, the motion time series was further reduced to a single scalar quantity by computing the mean value of the relative displacement vector, called the mean relative displacement (MRD).

Study sub-samples

In our complete sample of 780 subjects, subject motion declined with age as expected ($r = -0.19$; $p<0.001$, Figure 1A). Although our main group level analyses in the complete sample included motion as a confounding covariate (see below), we also conducted supplementary analyses in two specific sub-samples in which age and motion were uncorrelated (Figure 1).

As described below we selected a motion-matched subsample (n=729) and a nearly-motionless, motion-matched sub-sample (n=70). Matching is an alternative to including motion in the group-level regression model as a confounding covariate (Dosenbach et al., 2010; Satterthwaite et al., 2012; Satterthwaite et al., 2013). The age-motion uncorrelated sample was selected using a greedy matching algorithm (Carpenter, 1977) implemented in MATLAB. In each loop of the algorithm, the correlation between motion and age was calculated without each individual subject that still remained in the sample. This produced a distribution of correlation coefficients; the subject whose exclusion resulted in the lowest correlation between age and motion was removed from the sample. The algorithm stopped and samples were considered matched when the absolute *r* value was <0.01. This procedure produced an age-motion matched sample that included 729 subjects (mean age=15.9 years, S.D.=3.1, 306 male) where the correlation between age and motion was $r=-0.009$ (Figure 1B).

As a final step, in order to further bolster confidence in our findings, we examined a second sub-sample of subjects that was nearly-motionless. This sub-sample included subjects only if their maximum volume-to-volume displacement was <0.1mm. However, even using this criterion, age and motion were still significantly related ($r=-0.13$). Therefore, the matching algorithm described above was applied in order to ensure that age and motion were uncorrelated, producing a final sub-sample of n=70 subjects (mean age=16.8 years, S.D.=3.0, 31 male; mean subject MRD=0.0265mm, SD=0.005mm) where the correlation between age and motion was $r=-0.002$ (Figure 1C).

Network construction

We examined the effects of development within a system of 264 nodes described by Power et al. (2011). In this network, nodes are 5mm radius spheres in MNI space that were drawn from both meta-analysis of task fMRI studies and resting-state functional connectivity mapping techniques (Cohen et al., 2008; Nelson et al., 2010). Power et al. (2011) provide a parcellation scheme for these nodes that delineates 13 functional modules that correspond to known large-scale brain networks that are coherent during both task activity and at rest (Smith et al., 2009; Yeo et al., 2011). Within this system of 264 nodes, there are 34,716 unique edges. We selected this node system due to three main advantages. First, the nodes in the network cover the entire brain, providing a full range of inter-node distances, allowing us to investigate whether edgewise Euclidean distance is related to observed age effects after accounting for motion. Second, as the system has already been parsed into functional networks in a sample of adults (Power et al., 2011), it provides an independent reference to test the hypothesis that these networks will become more segregated with age, with increased intra-modular connectivity and diminished inter-modular connectivity. Third, the relatively high-dimensional nature of the data (34,716 unique edges) facilitates machine-learning approaches such as support vector regression, allowing us to test if functional connectivity can accurately predict subject age even after accounting for motion at the subject and group level.

Image registration

Subject-level BOLD images were co-registered to the T1 image using boundary-based registration (Greve and Fischl, 2009) with integrated distortion correction as implemented in FSL 5 (Jenkinson et al., 2012). Whole-head T1 images were registered to the Montreal Neurologic Institute 152 1mm template using the diffeomorphic SyN registration that is part of ANTS (Avants et al., 2008; Avants et al., 2011; Klein et al., 2009). All registrations were inspected manually and also evaluated for accuracy using spatial correlations. Network nodes were registered to subject space for timeseries extraction by concatenating the

coregistration, distortion correction, and normalization transformations so that only one interpolation was performed in the entire process.

Subject-level timeseries processing

A voxel-averaged timeseries was extracted from each of the 264 nodes for every subject. In order to evaluate the impact of motion, data was preprocessed using both standard confound regression as well as a validated confound regression procedure that has been optimized to reduce the influence of subject motion (Satterthwaite et al., 2013). In both cases, the first 4 volumes of the functional timeseries were removed to allow signal stabilization, leaving 120 volumes for subsequent analysis. Functional images were slice-time corrected and re-aligned using MCFLIRT (Jeknsion et al., 2002). Structural images were skull-stripped using BET (Smith, 2002) and segmented using FAST (Zhang et al., 2001); mean white matter (WM) and cerebrospinal fluid (CSF) signals were extracted from the tissue segments generated for each subject (Reetz et al., 2012; Jakobs et al., 2012). Standard confound regression included 9 parameters: mean global signal, mean WM signal, mean CSF signal, as well as six motion parameters (9 regressors total). Improved confound regression (Satterthwaite et al., 2013) included these 9 parameters as well as the temporal derivative, quadratic term, and temporal derivative of the quadratic of each (i.e., 36 regressors total; see Friston et al., 1996 for a similar application of quadratic motion regresssors to task-based fMRI). Furthermore, as described previously (Satterthwaite et al., 2013) motion-related spike regressors were included in the model whenever a volume-to-volume displacement was greater than 0.25mm. It should be noted that current methods of estimating motion through the use of timeseries realignment parameters do not allow one to attribute motion to a specific acquisition volume. Rather, motion can only be detected as a displacement (or change in relative position) from one volume to the next. Here, we included a single regressor for each volume bounding the observed displacement (i.e. TR −1 and TR +1); these spike regressors effectively censor the influence of these volumes in subsequent analysis of residual timeseries (Lemieux et al., 2007). As two volumes are lost from analysis for each spike, subjects with >20 spikes were excluded (see “Participants” above), ensuring that each subject had at least 4 minutes (80 volumes) of timeseries data for analysis (Van Dijk et al., 2010). Notably, subjects in the nearly-motionless sample had no volumes that were flagged for spike regression as all volume-to-volume displacements were <0.1mm. Following confound regression, residual timeseries were band-pass filtered to retain signals between 0.01–0.08 Hz (Satterthwaite et al., 2013). Finally, a symmetric connectivity matrix (264×264) was defined for each subject using pairwise Pearson’s correlations.

Network visualization

In order to aid visualization of the overall network structure, a mean connectivity matrix was created by averaging across all subjects. This average connectivity matrix was displayed in graphical form using a spring-embedded force-based rendering with Gephi (Bastian et al., 2009). In this representation, nodes that are tightly connected are brought closer together, whereas nodes that are not connected are pushed farther apart on the graph. As negative connections cannot be visualized effectively in such a graph, in this representation only positive values are displayed, with graph edges thresholded to produce a network density of 10% (Figure 2).

Group-level analyses: effect of age

As a first step, we investigated whether significant age effects on resting-state functional connectivity remain after rigorously accounting for motion at the subject and group level. Here and in subsequent analyses, we examined the effects of age on functional connectivity using four models in the complete sample (n=780):

M1 Standard (9-parameter) confound regression; motion (MRD) *not* included as a confounding covariate in the group-level analysis.

M2 Standard (9-parameter) confound regression; motion included as a confounding covariate in the group-level analysis.

M3 Improved (36-parameter + spike regression) confound regression; motion *not* included as a confounding covariate in the group-level analysis.

M4 Improved (36-parameter + spike regression) confound regression; motion included as a confounding covariate in the group-level analysis.

Furthermore, as an alternative to including motion as a confound regressor in the group level model, supplementary analyses were conducted in the age-motion matched sample (n=729) following both standard (M5) and improved confound regression (M6). For each condition, an across-subjects partial correlations were run at each of the 34,716 unique connections in the network, where functional connectivity was the dependent variable and age was the independent variable. Sex was a covariate included in all models; MRD was included as a confounding covariate only in models M2 and M4 as specified above. To provide a summary of the overall predominance of age-related connectivity change for a given approach, we report the number of connections with a significant age effect after controlling for multiple comparisons using a threshold determined by the false-discovery rate ($Q<0.05$; Genovese et al., 2002).

While the total number of connections that change with age provides an easily interpretable measure of the age effect, it does not provide an estimate of the overall magnitude of the age-connectivity relationship. Accordingly, as in our previous work (Satterthwaite et al., 2013), we also report the median absolute correlation between age and connectivity across all 34,716 unique graph edges. Individual models were compared with a Wilcoxon sign-rank test of the distributions of age-connectivity correlations. As described below in the results, substantial age effects persisted in all approaches; because visualizing the large number of significant edges present using an FDR ($Q<0.05$) threshold was impractical, only age effects that survived Bonferroni correction (corrected $p<0.05$; uncorrected $p<1.4\times10^{-6}$) are displayed. Network nodes and connections were visualized in three dimensions using custom software written in-house with Mayavi (Ramachandran and Varoquaux, 2011).

Evaluation of impact of global signal regression

It should be noted that the preprocessing steps outlined above include global signal regression (GSR). Prior work has shown that GSR may potentially bias results (Murphy et al. 2009; Saad et al., 2012; but also see Fox et al., 2009 and Yan et al., 2013). However, in our previous work we have shown that even small amounts of in-scanner motion results in large drops in the BOLD signal across the brain parenchyma (Satterthwaite et al., 2013; see Figure 3) that is well-modeled by the global signal. In order to demonstrate the effect of inclusion of the global signal (and related WM and CSF signals) in this sample, we re-processed the data under two additional conditions:

M7 Standard confound regression with 6 motion parameters, but *without* inclusion of global, WM, or CSF signals in the regression; motion (MRD) was *not* included as a confounding covariate in the group-level analysis.

M8 Improved confound regression with 24 motion parameters and spike regressors, but again *without* global, WM, or CSF signals included. As above motion was *not* included as a confounding covariate in the group-level analysis.

For each of these models, as in our prior work (Satterthwaite et al., 2013) in order to provide a summary of the impact of motion on connectivity, we calculated the median absolute

correlation between MRD and connectivity across all network connections. For comparison, we also calculated this metric for the matching models M1 and M3, which included the global signal (as well as WM / CSF). As displayed in Supplementary Figure 1 and predicted by prior results (Satterthwaite et al., 2013; see also Yan et al., 2013), without GSR the relationship between motion and connectivity was markedly higher: nearly all network connections had a significant relationship between connectivity and motion without GSR, and the median absolute correlation between motion and connectivity was substantially elevated (r=0.28 with 6-parameter confound regression, r=0.20 with 24-parameter confound regression). The correlation with motion in models that included the global signal was substantially lower (r=0.06 and 0.04, respectively). Accordingly, GSR was retained for all subsequent analyses.

Follow-up analysis in nearly-motionless sub-sample

As a final step, in order to verify that un-modeled motion was not driving apparent age-related effects, we examined age effects within the nearly-motionless sub- sample of subjects (n=70). Specifically, we compared the correlation between connectivity and age in the nearly-motionless sub-sample within the 725 connections identified as having a significant (FDR Q<0.05) age effect in the sample that had been analyzed using improved preprocessing and a motion covariate in the group level analyses (i.e., M4). The mean absolute value of the correlation with age in these edges was calculated in both the full sample and the nearly-motionless subsample using descriptive statistics. As described below, given the large number of multiple comparisons and the small effect sizes of the age-connectivity relationship, this sub-sample was underpowered to detect substantial age-connectivity effects when all connections were evaluated in this sub-sample alone.

Follow-up analysis of degree to which motion inflates estimates of age-related connectivity change

As described below (see Results) the above analyses demonstrate that subject- and group-level strategies used to mitigate the influence of motion artifact also reduce the apparent magnitude and significance of age-related changes in connectivity. However, these analyses do not directly establish that motion itself inflates estimates of age-related connectivity change. In order to illustrate this more directly, we compared the age-connectivity relationship in the nearly-motionless, motion-matched sub-sample of subjects (n=70) to 1,000 randomly selected sub-samples of 70 subjects where the total amount of motion and the age-motion relationship was not controlled. For each randomly selected sub-sample, we calculated the total number of individual connections that had a significant (FDR Q<0.05) relationship with age, as well as the median absolute correlation between age and connectivity across all unique connections. We compared the number of significant connections found in the nearly-motionless, motion-matched sub-sample to this distribution of 1,000 randomly chosen groups of subjects with a Wilcoxon signed-rank test. The median absolute correlation between age and motion in the nearly-motionless, motion-matched sub-sample was similarly compared using a one-sample t-test.

Analyses of sample size necessary to detect age-related connectivity changes

Analyses of the nearly-motionless, age-matched subsample of 70 subjects revealed that this sample was underpowered to detect widespread age-related change in connectivity. As typical studies of development are generally of a much smaller scale than the PNC, we conducted follow-up analyses using random sub-samples of our own data to ascertain what sample size was necessary to detect age-related changes in connectivity. First, in order to determine the relationship between sample size and the number of connections that would be expected to have an FDR-significant effect of age in a network of this size, we conducted a series of analyses using random sub-samples (without replacement) over a range of sample

sizes. Specifically, we evaluated sample sizes between 25 and 400 subjects at intervals of 25 subjects (e.g., n=25, n=50, etc.). For each sample size *n*, we selected *n* subjects 100 times from the available pool of 780 subjects. For each randomly selected sample, the number of FDR-corrected connections that exhibited a significant relationship with age was calculated for both model M1 (standard processing, no group-level motion covariate) and model M4 (improved preprocessing + group level motion covariate). At each sample size considered, the average number of FDR-significant connections was calculated over the 100 random samples evaluated. Lowess curves were constructed from the data or each processing approach; these curves summarize the extent of age-related connectivity change that can be expected to be found with a given sample size in a relatively high-dimensional whole-brain network.

Second, given the large number of multiple comparisons that require correction, smaller studies are less likely to conduct whole-brain exploratory analyses using a high-dimensional networks such as the one utilized here. Accordingly, we repeated the procedure outlined above but only examined a single connection between the posterior cingulate (PCC; MNI coordinates: −7, −55, 27) and the ventromedial prefrontal cortex (vMPFC; −7, 51, −1). The PCC and vMPFC are both major hubs of the default mode network (Andrews-Hannah et al., 2010, Schilbach et al., 2012; Van Dijk et al., 2010) and connectivity has previously been found to increase during development (Fair et al., 2008). Note that the age-connectivity relationship for this connection in the complete sample using model M4 was quite significant: $r=-0.15$, $p=3.02\times10^{-5}$. For this analysis, in each sub-sample considered, instead of calculating the number of FDR-corrected significant connections present within the entire network, we simply recorded whether this single PCC-vMPFC connection was significant at an uncorrected threshold of $p<0.05$. Because of the lower dimensionality of the data, we evaluated samples of 10–400 subjects at an interval of 1 subject. As 100 random sub-samples were evaluated for every sample size, the final outcome reported was the proportion of times that a significant effect was detected. As above, this analysis was completed for both models M1 and M4; lowess curves were again fit to the data. Finally, we report the number of subjects needed to find a significant age-related change in vMPFC-PCC connectivity 80% of the time.

Group-level analyses: impact of inter-node distance on effects of age

A commonly reported finding regarding the development of functional connectivity in childhood and adolescence is that long-range connectivity strengthens and short-range connectivity diminishes (Supekar et al., 2009; Dosenbach et al., 2010; Fair et al., 2007; Fair et al., 2009). However, as motion artifact can mimic this same pattern, we investigated the degree to which a distance-dependent effect remains after accounting for motion at the subject and group level. Data was analyzed in the four main model conditions outlined above (M1–M4) that used the entire sample (n=780); supplementary analyses considered the age-motion matched sub-samples (n=729; M5 & M6). Next, for each model condition the mean Euclidean distance of connections that showed a significant (FDR $Q<0.05$) age effect was calculated separately for connections that strengthened with age (age-positive) and those that weakened with age (age-negative). Within each model condition, the Euclidean distance of age-positive and age-negative connections were compared using a *t*-test. In order to directly compare models, the distance of age-positive connections for the improved preprocessing + group-level regression approach (M4) were compared to the other main models (M1–M3) using *t*-tests. This was repeated separately for significant age-negative connections. Finally, in order to provide an estimate of the degree to which inter-node distance modulated the effect of age on connectivity, we calculated the correlation between the z-transformed age-connectivity correlation and the inter-node Euclidean distance. This

analysis is quite analogous to our prior work examining the modulating effect of inter-node distance and the appearance of motion artifact itself (Satterthwaite et al., 2013).

Group-level analyses: age-related network segregation

A prominent finding in studies of developmental connectivity is that large-scale functional brain networks become more segregated from each other, with enhanced within-network connectivity and diminished between-network connectivity (Anderson et al., 2011; Fair et al., 2007; Fair et al., 2008; Fair et al., 2009; Supekar et al., 2009). We next evaluated the degree to which accounting for in-scanner motion impacts this effect. As above, data was evaluated following processing under the four main model conditions in the entire sample (n=780; M1–M4), as well as within the age-motion matched subsample (n=729, M5–M6). In order to provide an easily-interpretable measure of the degree to which connectivity within and between functional network modules relate to the effects of age, we calculated the percentage of connections that grow stronger with age that were within-network or between-network. This was also done separately for connections that grow weaker with age. (For reference, only 11% of the unique connections are within-module connections, whereas 89% are between-module connections.) In order to provide a statistical summary of the degree to which within-module connections and between-module connections differed among models, we compared the improved preprocessing + group-level regression (M4) approach to the other main models (M1–3) using a chi-square test. Specifically, we compared the proportion of significant age-positive connections that were within-module, and repeated this procedure to evaluate the proportion of within-module age-negative connections.

Prediction of subject age using multivariate pattern analysis

Finally, we tested whether the complex multivariate pattern of resting-state functional connectivity can be used to derive a “functional maturation index” that correlates highly with subject age (Dosenbach et al., 2010). To do this, the 34,716 unique edges for each subject were entered as features into a linear support vector regression (SVR) algorithm (Chang and Lin, 2011) and used to predict subject age. No feature selection was implemented prior to SVR. Predictions were generated using a 10-fold cross validation procedure with random subsampling where the multivariate model was trained on 90% of the data, and then tested on 10% of the data. This procedure provides an unbiased estimate of model predictive accuracy and prevents model over-fitting. Unlike multiple regression, SVR does not allow the inclusion of a covariate; accordingly, we examined age-matched and unmatched samples using both improved and standard confound preprocessing (i.e. M1, M3, M5, M6). Predictive abilities of models were summarized using a Pearson’s correlation, and compared via a Fisher’s r to z transformation.

As described below (see Results), SVR revealed that improved preprocessing and group-level matching resulted in significantly poorer predictive accurate than standard preprocessing and an unmatched group. In order to understand what drove this difference in predictive accuracy, we conducted 1,000 permutations for each model to identify significantly weighted model features. Overall permutation-based model significance is reported as well. As in the mass-univariate analysis, the mean Euclidean distance of significantly weighted features was calculated separately for age-positive and age-negative connections. The distance of age-positive and age-negative features was compared among models using two-sample t-tests.

Because Dosenbach et al. (2010) reported a non-linear relationship between the functional maturation index and age, we tested for non-linear effects using a flexible non-parametric multivariate adaptive regression spline model (Friedman, 1991) implemented in STATA

(StataCorp; College Station, TX). In this model actual age was regressed versus predicted age, using a procedure that directly compares a linear fit to higher-order spline models that do not assume a parametric function. As detailed by Royston and Sauerbrei (2007), the MVRS algorithm is an adaptation of the fractional polynomial approach and uses a similar closed-test procedure for evaluating model complexity. For all data, linear models are considered the default; the significance of the additional variance explained by splines was compared to the linear model using a likelihood ratio test.

RESULTS

Motion inflates estimates of age-related connectivity change, but these effects persist after controlling for motion

As a first step, we examined the degree to which procedures that account for motion artifact impact the presence of age-related connectivity change. Strategies that account for motion artifact on both the subject- and group-level clearly reduced the amount of apparent age-related changes in connectivity (Figure 3A, Figure S2). Following improved preprocessing and group-level covariation (M4), age effects were significantly reduced compared to all models. The distribution of absolute age-connectivity correlations in M4 was less than the next most-similar model (M3), z=10.8, $p < 1.0 \times 10^{-10}$ (Figure 3B). Nonetheless, age effects remain prominent after modeling motion at the subject- and group-level, even after stringent type-I error control with the Bonferroni correction (Figure 3C).

Furthermore, when the connections that were found to have a significant age effect in the most conservative model (M4) were examined in in the nearly-motionless, age-matched subsample of subjects (n=70), the absolute magnitude of the age-connectivity correlation was quite similar (i.e., r=0.16 in nearly-motionless sample versus r=0.13 in full sample), suggesting that un-modeled motion did not drive observed results. However, it should be noted that the effect size of the observed age-related changes in fact is small. As a result, analyses examining age-related changes across all unique edges in the nearly-motionless sub-sample revealed only a single connection that survived corrections for multiple comparisons. Thus, this sub-sample was not considered in the subsequent analyses that seek to parse the influence of motion on the significant age-related changes that were observed in the complete sample.

While the above results demonstrate that the relationship between motion and age is reduced by both improved preprocessing and accounting for motion in the group-level analysis, it does not directly demonstrate that motion itself inflates the age-connectivity relationship. Accordingly, we next compared the significance and magnitude of the relationship between connectivity and age in the nearly-motionless sub-sample of subjects (n=70) to 1,000 randomly selected sub-samples of 70 subjects where the total amount of motion and the age-motion relationship was not controlled. Notably, the number of unique graph edges where there was a significant age-connectivity relationship was lower in the nearly-motionless, sub-sample than the distribution of sub-samples where motion was not controlled (z=4.6, $p=4.13 \times 10^{-6}$). The median absolute correlation between age and connectivity was also significantly lower (t=28.5, $p<1 \times 10^{-10}$). Taken together, results show that while motion inflates apparent age-related changes in connectivity, such effects nonetheless remain widespread even after carefully accounting for subject motion.

Large samples are needed to detect significant age-related connectivity change

Notably, analysis of the nearly-motionless subsample of 70 subjects revealed only one connection that survived multiple comparison corrections using FDR (Q<0.05). This suggests that such a sample size may be underpowered to detect significant age-related

changes in connectivity. As typical studies of development are generally of a smaller scale than the PNC, we conducted additional analyses using random sub-samples of our own data to ascertain what sample size would be necessary to detect age-related changes in connectivity. This analysis revealed that after accounting for motion with improved preprocessing and group-level covariation (model M4) 275 subjects would be needed to on average detect 10 network edges that survive FDR correction. In contrast, only 100 subjects analyzed using model M1 would reveal a similar number of significant connections. As seen in Supplementary Figure 3A, the prevalence of age-related findings produced by the two approaches diverges sharply as sample sizes increase.

Next, given the large number of multiple comparisons that require correction in this network, we conducted a second analysis of a single PCC-vMPFC connection. This analysis indicated that a sample size of 182 subjects would be necessary to detect significant age-related strengthening of these two default mode hubs 80% of the time using model M4 (Figure S3B). In contrast, 140 subjects would be equally powered to produce significant results if model M1 was used.

Motion exaggerates distance-dependent age effects

Next, we investigated the degree to which previously-reported relationships between inter-node distance and age were present after accounting for motion. Consistent with prior reports, distance effects were quite marked when data was analyzed using standard methods (Figure 4A). Specifically, connections that became stronger with age (age-positive) were longer-range than those that became weaker with age (age-negative). However, both subject-level and group-level correction strategies clearly diminished this effect (Figure 4A, Figure S4), with the improved-preprocessing, group-level covariation approach (M4) having significantly shorter age-positive connections (t=2.86, p=0.004) than the next-most similar model (M3). The inter-node distance of age-negative connections was not different between models M4 and M3 or M4 and M2; however, age-negative connections were significantly longer in model M4 than M1 (t=3.17, p=0.001). Nonetheless, even following both improved preprocessing and group-level covariation (M4), age-positive connections remained significantly longer range than age-negative connections (t=3.07, p=0.002; Figure 4A & 4B).

The above analyses only considered the inter-node distance of significant age-positive and age-negative connections. Next, we examined the modulating effect of inter-node distance on the age-connectivity relationship across all graph connections. As seen in Figure 4C, with standard preprocessing and no group-level correction (model M1), there was a substantial (r=0.21) association between internode distance and the age-connectivity correlation. Notably, both improved preprocessing and group level covariation (as well as matching) almost erased this relationship (i.e., r=0.01 for model M4).

Increase in intra-modular connections with development is enhanced when accounting for motion

Results thus far suggest that motion serves to inflate age- and distance-related effects observed in studies of developmental functional connectivity. We next investigated the effect of motion on developmental changes in network segregation by examining the relative strength of within-module versus between-module connectivity. As expected, using standard processing methods (model M1) we found that age-positive connections were more likely to be within-module than age-negative connections (Figure 5A, Figure S5). However, in contrast to the attenuating effect of motion-control strategies on associations with inter-node distance, we found that accounting for motion in fact enhanced the effect of network segregation with age: the proportion of age-positive connections that were within-module

increased with improved preprocessing. Both improved preprocessing with and without group-level covariation of motion (M3 and M4) had a higher proportion of within-module connections compared to models using standard confound regression (i.e., M1 and M2). Specifically, when improved preprocessing + group level covariation (M4) was compared to standard preprocessing + group level covariation (M2), the difference was highly significant: χ^2= 34.5 p=4.2×10^{-9}. Overall, this pattern is the inverse of what was observed in the analysis of inter-node distance, as accounting for motion actually strengthens specific age-related effects of network segregation. Age-negative connections were also somewhat more likely to be within-module with both subject- and group-level control of motion; improved preprocessing and group-level covariation (M4) had a higher proportion of within-module age-negative connections compared to model M1 (χ^2=5.1, p=0.02); no other model was significantly different for age-negative connections. At a very high threshold for significance (using Bonferroni correction), connections that strengthen with age are mainly intra-modular, whereas connections that weaken with age are much more likely to be between-module (Figure 5B). Overall, motion attenuated the appearance of network segregation with age, and accounting for motion strengthened this effect.

Multivariate patterns of functional connectivity remain highly predictive of subject age

The above results demonstrate that uncontrolled motion inflates the modulation of age-related changes in connectivity by inter-node distance, but obscures specific age-related changes in large-scale network structure. We next examined the degree to which motion-control strategies impact the ability to derive a functional maturation index of brain development using multivariate pattern-regression methods (i.e., SVR). We found that the correlation between subject age and the predicted multivariate functional maturation index was diminished when both improved preprocessing and group-level matching was applied (Figure 6A). Standard preprocessing and no matching (model M1) resulted in a correlation between actual and predicted age of 0.62; this was significantly better than the prediction yielded by improved preprocessing and group-level matching (model M6; r=0.50, Figure 6B; M1 vs. M4: z=3.5, p=0.0005). Nonetheless, this degree of accuracy for model M4 remained highly significant (permutation-based p<0.001). Other models yielded intermediate prediction values and were not significantly different from each other. As expected, significantly weighted connections that weakened with age from model M1 were shorter than those from model M6 (t=2.36; p=0.02); there was also trend towards significantly-weighted age-positive features being longer in M1 than M6 (p=0.08). When actual versus predicted age was compared using multivariate regression splines in model M6, a linear fit was found to be more appropriate than a non-linear spline.

DISCUSSION

Here we demonstrate that motion has a heterogeneous impact on measured changes in functional connectivity during development in youth. Motion inflates overall estimates of age-related changes in functional connectivity as well as the dependence of this effect on inter-node distance. Conversely, motion attenuates measures reflecting increased network segregation over development. After accounting for motion effects, the complex pattern of functional connectivity can still predict an individual subject's age with a high degree of accuracy using multivariate pattern regression. Accounting for motion artifact therefore reduces certain patterns of age-related connectivity change but enhances others, and is more likely to yield valid estimates of the evolving neurobiology of development.

Motion inflates estimates of age and distance-dependent connectivity change

The first question we set out to answer in this study was whether age-related changes in connectivity remained after rigorously controlling for the influence of motion artifact. Our

results clearly demonstrate that motion inflates the appearance of age-related connectivity change. Indeed, whereas 14% of pair-wise connections appeared to have a significant age effect using standard procedures, this was reduced to only 2% after more rigorous correction for motion at the subject- and group-level. Nonetheless, even after such a conservative analytic approach, it is equally clear that connectivity does change substantially during development. Observed age-related differences remain significant beyond conservative statistical thresholds for type I error control (i.e., Bonferroni correction), and examination of these connections in a nearly-motionless sub-sample reveals age-related changes of a similar effect size.

It should be noted, however, that the effect size (approximately r=0.13) of such age-related changes is in fact small: FDR-corrected results in a high-dimensional network like the one utilized here (Power et al., 2011) only become consistently apparent in samples that contain at least approximately 275 subjects. As expected, testing an *a priori* requires somewhat fewer subjects: 182 subects are required to detect a simple strengthening of connectivity between the default mode hubs of the PCC and vMPFC with 80% reliability. This suggests that resting-state studies of neurodevelopment in youth using typical sample sizes (e.g., 30–100 subjects) are substantially underpowered for exploratory analysis of high-dimensional networks, and (in combination with the presence of uncontrolled motion artifact) may explain the heterogeneous results of some prior studies. The large sample sizes required emphasize the need for large-scale multi-modal imaging initiatives such as the PNC, the Pediatric Imaging, Neurocognition, and Genetics Study (PING; Brown et al., 2012), and the IMAGEN consortium (Schumann et al., 2010). Establishing the PNC as a publicly available resource for the study of brain development was one of the principal aims of this initiative. As noted elsewhere (Biswal et al., 2010; Gorgolewski et al., 2013; Mennes et al., 2012; Milham, 2012; Nooner et al., 2012), data sharing is a prerequisite for the collaboration necessary to gain traction towards understanding complex phenomena such as the neurodevelopmental origins of psychiatric illness. These results also reinforces that multivariate methods that integrate disparate individual effects of small effect sizes to produce more robust results are of great utility, as discussed below.

Motion obscures age-related changes in within-network connectivity

While motion inflates overall estimates of age-related changes as well as the impact of inter-node distance, in-scanner motion was also found to have the opposite effect in attenuating the pattern of network segregation with age. When processed using standard methods and without group-level covariation, previously-reported patterns of age-related change in connectivity were apparent: connections that grew stronger with age were more likely to be within-module than connections that grew weaker with age (the vast majority of which were between-module). Notably, controlling for motion at both the timeseries and group level robustly increased the proportion of age-positive connections that were within-module. As previously noted, this finding suggests that large-scale brain networks become increasingly differentiated with age (Anderson et al., 2011; Dosenbach et al., 2010; Fair et al., 2007; Fair et al., 2009; Supekar et al., 2009), which may contribute to the improvements in cognitive capabilities that occur during development (Kelly et al., 2008). We show that motion tends to mask this developmental phenotype, which could be important for understanding individual brain-behavior differences as well as developmental pathophysiology.

Multivariate prediction of subject age remains accurate even when accounting for motion

In a prominent study of neurodevelopment, Dosenbach et al. (2010) found that complex, multivariate patterns of connectivity could be used to predict a subject's age with a high degree of accuracy, suggesting that connectivity can provide a useful measure of functional brain maturation. While that study used samples where age and motion were unrelated,

motion was only accounted for at the subject-level using standard (6-parameter) motion regression. Our results demonstrate that, as predicted by the mass-univariate results, accounting for motion reduces the accuracy of multivariate predictions of subject age. Examination of significantly-weighted model features revealed that this is in part because distance-dependent effects that were more heavily weighted using standard methods were less prominent following greater control of motion artifact through group-matching and improved confound regression. Nonetheless, it should be noted that while better control of motion did reduce predictive accuracy to some degree, it remained high: predicted age was correlated with actual age r=0.5 even following improved preprocessing and an age/motion matched sample. Also, in contrast to Dosenbach et al., we found a linear relationship between multivariate patterns of connectivity and subject age. However, compared to the age range in the present sample (8–22 years old), Dosenbach et al. included a substantially wider range (5–30 years old) and nonlinearities in that study only became apparent above age 20. Overall, our results buttress the prior findings of Dosenbach et al., and emphasize that functional connectivity remains a valuable phenotype for charting trajectories of neurodevelopment.

Limitations and future directions

While this study leverages a very large sample and carefully examines the impact of motion artifact on age-related changes in connectivity, certain limitations should be acknowledged. First, although improved confound regression mitigates the influence of motion artifact on connectivity, it does not completely abolish it (Satterthwaite et al., 2013). In the future, techniques such as automated labeling of motion-related components generated by single-subject independent components analysis (ICA) may provide better separation of motion-related noise from true connectivity signal (Beckmann et al., 2005). Second, because subject-level timeseries processing could not fully remove the influence of motion, we additionally accounted for the influence of motion as part of the group level analysis. As we have previously noted (Satterthwaite et al., 2012; Satterthwaite et al., 2013), such a covariation approach has the disadvantage of reducing sensitivity in proportion to the degree to which motion and the variable of interest (i.e. age) are correlated. While matching motion and age is a suitable alternative, it may bias the study population by selecting for abnormally still children and abnormally movement-prone adults. Third, better control of motion artifact may be provided by external monitoring of motion (Tremblay et al., 2005), which may offer more accurate measures of in-scanner motion than the realignment parameters used here, and potentially allow on-line correction of artifact (Maclaren et al., 2012). Fourth, modifications to pulse sequences including using dual-echo imaging acquisition techniques may help reduce the impact of motion artifact on BOLD signal (Ing and Schwarzbauer, 2012). Fifth, the increasing availability of multiplex EPI acquisitions with sub-second TR (Feinberg et al., 2010) may allow for better control of motion artifact by preventing the aliasing of higher-frequency motion-related signals into lower frequencies that provide greater contributions to functional connectivity. Finally, it should be noted that in the present work we evaluated changes in connectivity within a system of large-scale brain networks defined in a sample of adults by Power et al. (2011). One limitation of this approach is that it does not allow us to describe how the community structure of these networks develops during adolescence; this remains a fertile ground for future research. In particular, modular degeneracy (Rubinov and Sporns, 2011) and the overlapping brain networks described by sparse dictionary learning (Eavani et al., 2012) may be a powerful framework for describing this evolution.

Conclusions

Here, we re-evaluated the most prominent findings in neurodevelopmental connectivity after accounting for motion artifact. We found that motion inflates the general appearance of age-

related connectivity change as well as their apparent relation to inter-node distance. In contrast, motion attenuates evolving patterns of network segregation, and controlling for motion makes this effect more obvious. Finally, complex multivariate patterns of connectivity remain highly predictive of subject age even after controlling for subject motion. On the balance, while these results demonstrate that certain aspects of previously-published findings may have been biased by motion artifact, they suggest that motion artifact alone cannot completely explain such results, and that existing conceptions of fundamental patterns of neurodevelopmental change in connectivity can be maintained. While studies of neurodevelopment using resting state functional connectivity remain particularly prone to contamination by motion artifact given the strong relationship between subject age and in-scanner motion, this problem is not unique to neurodevelopmental research and also applies to studies of psychopathology and individual differences, where the independent variable is often strongly correlated with in-scanner motion. Taken together, the present results argue that functional connectivity remains a valuable phenotype for the study of neurodevelopment, which may be assessed with greater accuracy when carefully controlling for motion.

Supplementary Material

Refer to Web version on PubMed Central for supplementary material.

Acknowledgments

Many thanks to the acquisition and recruitment team: Marisa Riley, Jack Keefe, Nick DeLeo, Raphael Gerraty, Elliott Yodh, and Rosetta Chiavacci. Thanks to Ewald Moser for discussion.

FINANCIAL SUPPORT: Supported by grants from the National Institute of Mental Health MH089983, MH089924, and T32 MH019112. Dr. Satterthwaite was supported by NIMH K23MH098130, APIRE, and NARSAD through the Marc Rapport Family Investigator Grant. Dr. Wolf was supported by NIMH K23MH085096, APIRE, and NARSAD through the Sidney R. Baer, Jr. Foundation. Dr. Eickhoff was supported by the Human Brain Project (R01-MH074457-01A1) and the Helmholtz Initiative on Systems Biology (Human Brain Model).

References

Anderson JS, Ferguson MA, Lopez-Larson M, Yurgelun-Todd D. Connectivity gradients between the default mode and attention control networks. Brain Connect. 2011; 1:147–157. [PubMed: 22076305]

Andrews-Hanna JR, Reidler JS, Sepulcre J, Poulin R, Buckner RL. Functional-anatomic fractionation of the brain's default network. Neuron. 2010; 65:550–562. [PubMed: 20188659]

Avants BB, Epstein CL, Grossman M, Gee JC. Symmetric diffeomorphic image registration with cross-correlation: evaluating automated labeling of elderly and neurodegenerative brain. Med Image Anal. 2008; 12:26–41. [PubMed: 17659998]

Avants BB, Tustison NJ, Song G, Cook PA, Klein A, Gee JC. A reproducible evaluation of ANTs similarity metric performance in brain image registration. Neuroimage. 2011; 54:2033–2044. [PubMed: 20851191]

Bastian M, Heymann S, Jacomy M. Gephi: An open source software for exploring and manipulating networks. 2009

Beckmann CF, DeLuca M, Devlin JT, Smith SM. Investigations into resting-state connectivity using independent component analysis. Philos Trans R Soc Lond B Biol Sci. 2005; 360:1001–1013. [PubMed: 16087444]

Biswal B, Yetkin FZ, Haughton VM, Hyde JS. Functional connectivity in the motor cortex of resting human brain using echo-planar MRI. Magn Reson Med. 1995; 34:537–541. [PubMed: 8524021]

Biswal BB, Mennes M, Zuo XN, Gohel S, Kelly C, Smith SM, Beckmann CF, Adelstein JS, Buckner RL, Colcombe S, Dogonowski AM, Ernst M, Fair D, Hampson M, Hoptman MJ, Hyde JS,

Kiviniemi VJ, Kötter R, Li SJ, Lin CP, Lowe MJ, Mackay C, Madden DJ, Madsen KH, Margulies DS, Mayberg HS, McMahon K, Monk CS, Mostofsky SH, Nagel BJ, Pekar JJ, Peltier SJ, Petersen SE, Riedl V, Rombouts SA, Rypma B, Schlaggar BL, Schmidt S, Seidler RD, Siegle GJ, Sorg C, Teng GJ, Veijola J, Villringer A, Walter M, Wang L, Weng XC, Whitfield-Gabrieli S, Williamson P, Windischberger C, Zang YF, Zhang HY, Castellanos FX, Milham MP. Toward discovery science of human brain function. Proc Natl Acad Sci U S A. 2010; 107:4734–4739. [PubMed: 20176931]

Carp J. Optimizing the order of operations for movement scrubbing: Comment on Power et al. Neuroimage. 2011; 76:436–438. [PubMed: 22227884]

Carpenter RG. Matching when covariables are normally distributed. Biometrika. 1977; 64:299–307.

Casey BJ, Jones RM, Hare TA. The Adolescent Brain. Annals of the New York Academy of Sciences. 2008; 1124:111–126. [PubMed: 18400927]

Chang CC, Lin CJ. LIBSVM: a library for support vector machines. ACM Transactions on Intelligent Systems and Technology (TIST). 2011; 2:27.

Cohen AL, Fair DA, Dosenbach NUF, Miezin FM, Dierker D, Van Essen DC, Schlaggar BL, Petersen SE. Defining functional areas in individual human brains using resting functional connectivity MRI. Neuroimage. 2008; 41:45–57. [PubMed: 18367410]

Deen, B.; Pelphrey, K. Outlook: Autism. www.sfari.org

Dosenbach NUF, Nardos B, Cohen AL, Fair DA, Power JD, Church JA, Nelson SM, Wig GS, Vogel AC, Lessov-Schlaggar CN, Barnes KA, Dubis JW, Feczko E, Coalson RS, Pruett JR, Barch DM, Petersen SE, Schlaggar BL. Prediction of individual brain maturity using fMRI. Science. 2010; 329:1358–1361. [PubMed: 20829489]

Eavani H, Filipovych R, Davatzikos C, Satterthwaite TD, Gur RE, Gur RC. Sparse Dictionary Learning of Resting State fMRI Networks. PRNI: International Conference on Pattern Recognition in Neuroimaging. 2012

Fair DA, Cohen AL, Dosenbach NUF, Church JA, Miezin FM, Barch DM, Raichle ME, Petersen SE, Schlaggar BL. The maturing architecture of the brain's default network. Proceedings of the National Academy of Sciences. 2008; 105:4028.

Fair DA, Cohen AL, Power JD, Dosenbach NUF, Church JA, Miezin FM, Schlaggar BL, Petersen SE. Functional brain networks develop from a "local to distributed" organization. PLoS Comput Biol. 2009; 5:e1000381. [PubMed: 19412534]

Fair DA, Dosenbach NUF, Church JA, Cohen AL, Brahmbhatt S, Miezin FM, Barch DM, Raichle ME, Petersen SE, Schlaggar BL. Development of distinct control networks through segregation and integration. Proc Natl Acad Sci U S A. 2007; 104:13507–13512. [PubMed: 17679691]

Feinberg DA, Moeller S, Smith SM, Auerbach E, Ramanna S, Gunther M, Glasser MF, Miller KL, Ugurbil K, Yacoub E. Multiplexed echo planar imaging for sub-second whole brain FMRI and fast diffusion imaging. PLoS One. 2010; 5:e15710. [PubMed: 21187930]

Fox MD, Raichle ME. Spontaneous fluctuations in brain activity observed with functional magnetic resonance imaging. Nat Rev Neurosci. 2007; 8:700–711. [PubMed: 17704812]

Fox MD, Zhang D, Snyder AZ, Raichle ME. The global signal and observed anticorrelated resting state brain networks. J Neurophysiol. 2009; 101:3270–3283. [PubMed: 19339462]

Friedman JH. Multivariate adaptive regression splines. The annals of statistics. 1991:1–67.

Friston KJ, Holmes A, Poline JB, Price CJ, Frith CD. Detecting activations in PET and fMRI: levels of inference and power. Neuroimage. 1996; 4:223–235. [PubMed: 9345513]

Genovese CR, Lazar NA, Nichols T. Thresholding of statistical maps in functional neuroimaging using the false discovery rate. Neuroimage. 2002; 15:870–878. [PubMed: 11906227]

Gorgolewski KJ, Margulies DS, Milham MP. Making data sharing count: a publication-based solution. Front Neurosci. 2013; 7:9. [PubMed: 23390412]

Greve DN, Fischl B. Accurate and robust brain image alignment using boundary-based registration. Neuroimage. 2009; 48:63–72. [PubMed: 19573611]

Gur RC, Richard J, Calkins ME, Chiavacci R, Hansen JA, Bilker WB, Loughead J, Connolly JJ, Qiu H, Mentch FD, Abou-Sleiman PM, Hakonarson H, Gur RE. Age group and sex differences in performance on a computerized neurocognitive battery in children age 8–21. Neuropsychology. 2012; 26:251–265. [PubMed: 22251308]

Ing A, Schwarzbauer C. A dual echo approach to motion correction for functional connectivity studies. Neuroimage. 2012; 63:1487–1497. [PubMed: 22846657]

Insel TR. Translating scientific opportunity into public health impact: a strategic plan for research on mental illness. Arch Gen Psychiatry. 2009; 66:128–133. [PubMed: 19188534]

Jakobs O, Langner R, Caspers S, Roski C, Cieslik EC, Zilles K, Laird AR, Fox PT, Eickhoff SB. Across-study and within-subject functional connectivity of a right temporo-parietal junction subregion involved in stimulus-context integration. Neuroimage. 2012; 60:2389–2398. [PubMed: 22387170]

Jenkinson M, Bannister P, Brady M, Smith S. Improved optimization for the robust and accurate linear registration and motion correction of brain images. Neuroimage. 2002; 17:825–841. [PubMed: 12377157]

Jenkinson M, Beckmann CF, Behrens TEJ, Woolrich MW, Smith SM. FSL. Neuroimage. 2012; 62:782–790. [PubMed: 21979382]

Kelly AMC, Uddin LQ, Biswal BB, Castellanos FX, Milham MP. Competition between functional brain networks mediates behavioral variability. Neuroimage. 2008; 39:527–537. [PubMed: 17919929]

Klein A, Andersson J, Ardekani BA, Ashburner J, Avants B, Chiang MC, Christensen GE, Collins DL, Gee J, Hellier P, Song JH, Jenkinson M, Lepage C, Rueckert D, Thompson P, Vercauteren T, Woods RP, Mann JJ, Parsey RV. Evaluation of 14 nonlinear deformation algorithms applied to human brain MRI registration. Neuroimage. 2009; 46:786–802. [PubMed: 19195496]

Lemieux L, Salek-Haddadi A, Lund TE, Laufs H, Carmichael D. Modelling large motion events in fMRI studies of patients with epilepsy. Magn Reson Imaging. 2007; 25:894–901. [PubMed: 17490845]

Luna B. Developmental changes in cognitive control through adolescence. Adv Child Dev Behav. 2009; 37:233–278. [PubMed: 19673164]

Maclaren J, Armstrong BSR, Barrows RT, Danishad KA, Ernst T, Foster CL, Gumus K, Herbst M, Kadashevich IY, Kusik TP, Li Q, Lovell-Smith C, Prieto T, Schulze P, Speck O, Stucht D, Zaitsev M. Measurement and correction of microscopic head motion during magnetic resonance imaging of the brain. PLoS One. 2012; 7:e48088. [PubMed: 23144848]

Nelson SM, Cohen AL, Power JD, Wig GS, Miezin FM, Wheeler ME, Velanova K, Donaldson DI, Phillips JS, Schlaggar BL, Petersen SE. A parcellation scheme for human left lateral parietal cortex. Neuron. 2010; 67:156–170. [PubMed: 20624599]

Mennes M, Biswal BB, Castellanos FX, Milham MP. Making data sharing work: The FCP/INDI experience. Neuroimage. 2012

Milham MP. Open neuroscience solutions for the connectome-wide association era. Neuron. 2012; 73:214–218. [PubMed: 22284177]

Murphy K, Birn RM, Handwerker DA, Jones TB, Bandettini PA. The impact of global signal regression on resting state correlations: are anti-correlated networks introduced? Neuroimage. 2009; 44:893–905. [PubMed: 18976716]

Nooner KB, Colcombe SJ, Tobe RH, Mennes M, Benedict MM, Moreno AL, Panek LJ, Brown S, Zavitz ST, Li Q, Sikka S, Gutman D, Bangaru S, Schlachter RT, Kamiel SM, Anwar AR, Hinz CM, Kaplan MS, Rachlin AB, Adelsberg S, Cheung B, Khanuja R, Yan C, Craddock CC, Calhoun V, Courtney W, King M, Wood D, Cox CL, Kelly AM, Di Martino A, Petkova E, Reiss PT, Duan N, Thomsen D, Biswal B, Coffey B, Hoptman MJ, Javitt DC, Pomara N, Sidtis JJ, Koplewicz HS, Castellanos FX, Leventhal BL, Milham MP. The NKI-Rockland Sample: A Model for Accelerating the Pace of Discovery Science in Psychiatry. Front Neurosci. 2012; 6:152. [PubMed: 23087608]

Paus T, Keshavan M, Giedd JN. Why do many psychiatric disorders emerge during adolescence? Nat Rev Neurosci. 2008; 9:947–957. [PubMed: 19002191]

Power JD, Fair DA, Schlaggar BL, Petersen SE. The development of human functional brain networks. Neuron. 2010; 67:735–748. [PubMed: 20826306]

Power JD, Barnes KA, Snyder AZ, Schlaggar BL, Petersen SE. Spurious but systematic correlations in functional connectivity MRI networks arise from subject motion. Neuroimage. 2012; 59:2142–2154. [PubMed: 22019881]

Power JD, Barnes KA, Snyder AZ, Schlaggar BL, Petersen SE. Steps toward optimizing motion artifact removal in functional connectivity MRI; a reply to Carp. Neuroimage. 2012b

Ramachandran P, Varoquaux G. Mayavi: 3D visualization of scientific data. Computing in Science & Engineering. 2011; 13:40–51.

Reetz K, Dogan I, Rolfs A, Binkofski F, Schulz JB, Laird AR, Fox PT, Eickhoff SB. Investigating function and connectivity of morphometric findings--exemplified on cerebellar atrophy in spinocerebellar ataxia 17 (SCA17). Neuroimage. 2012; 62:1354–1366. [PubMed: 22659444]

Royston, Sauerbrei. Multivariable modeling with cubic regression splines: A principled approach. Stata Journal. 2007; 7(1):45–70.

Rubinov M, Sporns O. Weight-conserving characterization of complex functional brain networks. Neuroimage. 2011; 56:2068–2079. [PubMed: 21459148]

Saad ZS, Gotts SJ, Murphy K, Chen G, Jo HJ, Martin A, Cox RW. Trouble at rest: how correlation patterns and group differences become distorted after global signal regression. Brain Connect. 2012; 2:25–32. [PubMed: 22432927]

Satterthwaite TD, Elliott MA, Gerraty RT, Ruparel K, Loughead J, Calkins ME, Eickhoff SB, Hakonarson H, Gur RC, Gur RE, Wolf DH. An improved framework for confound regression and filtering for control of motion artifact in the preprocessing of resting-state functional connectivity data. Neuroimage. 2013; 64:240–256. [PubMed: 22926292]

Satterthwaite TD, Wolf DH, Loughead J, Ruparel K, Elliott MA, Hakonarson H, Gur RC, Gur RE. Impact of in-scanner head motion on multiple measures of functional connectivity: Relevance for studies of neurodevelopment in youth. Neuroimage. 2012; 60:623–632. [PubMed: 22233733]

Schilbach L, Bzdok D, Timmermans B, Fox PT, Laird AR, Vogeley K, Eickhoff SB. Introspective minds: using ALE meta-analyses to study commonalities in the neural correlates of emotional processing, social & unconstrained cognition. PLoS One. 2012; 7:e30920. [PubMed: 22319593]

Smith SM. Fast robust automated brain extraction. Hum Brain Mapp. 2002; 17:143–155. [PubMed: 12391568]

Smith SM, Fox PT, Miller KL, Glahn DC, Fox PM, Mackay CE, Filippini N, Watkins KE, Toro R, Laird AR, Beckmann CF. Correspondence of the brain's functional architecture during activation and rest. Proc Natl Acad Sci U S A. 2009; 106:13040–13045. [PubMed: 19620724]

Somerville LH, Casey BJ. Developmental neurobiology of cognitive control and motivational systems. Curr Opin Neurobiol. 2010; 20:236–241. [PubMed: 20167473]

Supekar K, Musen M, Menon V. Development of large-scale functional brain networks in children. PLoS Biol. 2009; 7:e1000157. [PubMed: 19621066]

Tremblay M, Tam F, Graham SJ. Retrospective coregistration of functional magnetic resonance imaging data using external monitoring. Magn Reson Med. 2005; 53:141–149. [PubMed: 15690513]

Van Dijk KRA, Hedden T, Venkataraman A, Evans KC, Lazar SW, Buckner RL. Intrinsic functional connectivity as a tool for human connectomics: theory, properties, and optimization. J Neurophysiol. 2010; 103:297–321. [PubMed: 19889849]

Van Dijk KR, Hedden T, Venkataraman A, Evans KC, Lazar SW, Buckner RL. Intrinsic functional connectivity as a tool for human connectomics: theory, properties, and optimization. J Neurophysiol. 2010; 103:297–321. [PubMed: 19889849]

Van Dijk KRA, Sabuncu MR, Buckner RL. The influence of head motion on intrinsic functional connectivity MRI. Neuroimage. 2011; 59:431–438. [PubMed: 21810475]

Wang L, Su L, Shen H, Hu D. Decoding lifespan changes of the human brain using resting-state functional connectivity MRI. PLoS One. 2012; 7:e44530. [PubMed: 22952990]

Yan CG, Cheung B, Kelly C, Colcombe S, Craddock RC, Di Martino A, Li Q, Zuo XN, Castellanos FX, Milham MP. A comprehensive assessment of regional variation in the impact of head micromovements on functional connectomics. Neuroimage. 2013; 76C:183–201. [PubMed: 23499792]

Yeo BTT, Krienen FM, Sepulcre J, Sabuncu MR, Lashkari D, Hollinshead M, Roffman JL, Smoller JW, Zöllei L, Polimeni JR, Fischl B, Liu H, Buckner RL. The organization of the human cerebral cortex estimated by intrinsic functional connectivity. J Neurophysiol. 2011; 106:1125–1165. [PubMed: 21653723]

Zhang Y, Brady M, Smith S. Segmentation of brain MR images through a hidden Markov random field model and the expectation-maximization algorithm. IEEE Trans Med Imaging. 2001; 20:45–57. [PubMed: 11293691]

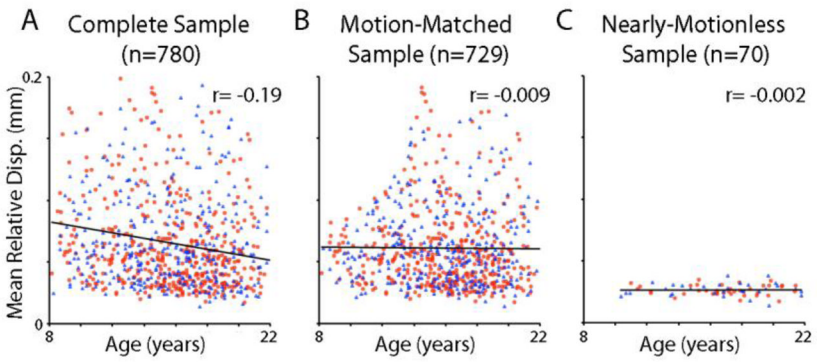

Figure 1.

Relationship between age and in-scanner motion in complete sample (**A**), a motion–matched sub-sample (**B**), and in a motion-matched, nearly-motionless sub-sample (**C**). Males are marked in blue, females are marked in red.

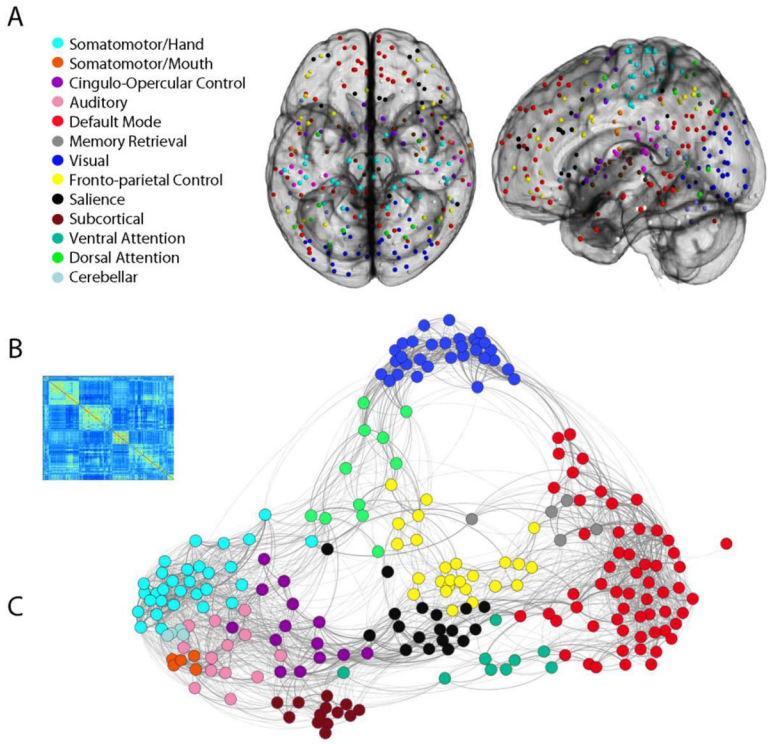

Figure 2.

Network definition. (**A**) Nodes in the network are defined according to the system established by Power et al. (2011), including 264 spheres (5mm radius) comprising 13 functional brain modules. Nodes are colored according to module membership as indicated in the figure legend. Nodes not assigned to a functional module by Power et al., (2011) are not displayed. (**B**) Mean network connectivity across full sample of 780 subjects displayed as a heat map. (**C**) Spring-embedded rendering of mean network connectivity matrix. Although all analyses are conducted using fully-connected networks with both positive and negative weights, for display graph edges are thresholded to produce a network density of 10%. Graph edge thickness is scaled according to connection strength. Nodes are colored by module assignment as in (**A**). As noted by Power et al. (2011), certain network modules (motor, visual, default) are more segregated, whereas networks implicated in cognitive control (frontoparietal, salience) display more inter-modular connections.

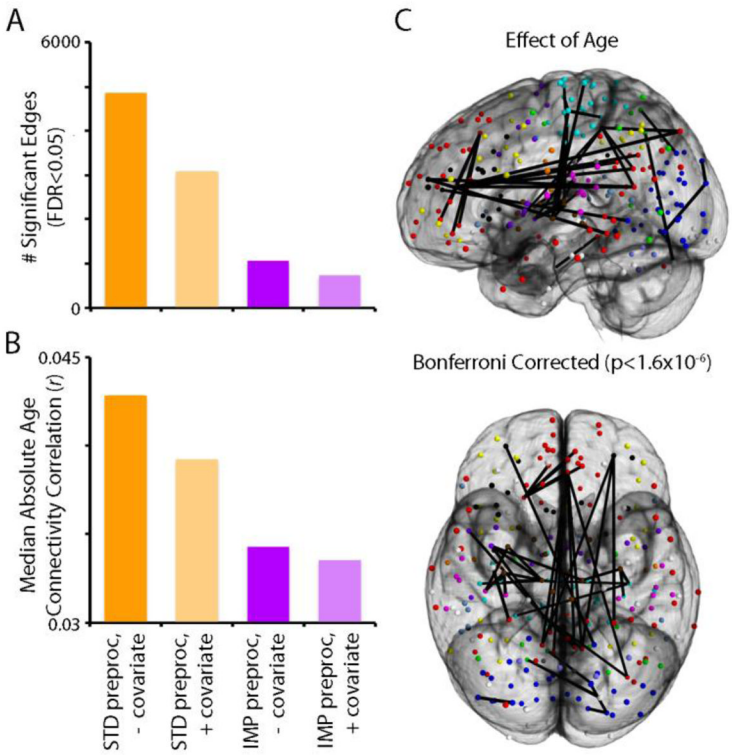

Figure 3.

Accounting for motion reduces but does not eliminate significant relationships between age and functional connectivity. (**A**) Number of statistically significant connections (FDR Q<0.05) within network of 264 nodes with 34,716 unique edges resulting from four different analysis procures, varying factors of subject-level confound regression and group-level covariation of motion. Standard confound regression included 9 parameters (6 motion parameters + global, WM, CSF timecourses); improved confound regression included 36 parameters (i.e., standard parameters + their temporal derivatives, quadratic terms, and quadratic of derivative) as well as spike regressors for relative displacements >0.25mm. Age effects were investigated at the group level either without a motion covariate or with motion (mean relative displacement) added as a covariate. Sex was included as a covariate in all models. (**B**) Similar results are seen when the median absolute correlation between age and connectivity is evaluated across models: age effects are diminished when motion is controlled for at the subject and group level. As the median is a robust representation of the central tendency of this skewed distribution, small changes in median connectivity here are accompanied by substantial changes in the tail of the distribution and the corresponding number of FDR-corrected significant connections (see **A**). (**C**) Graphical representation of the 42 connections that displayed significant age effects following improved preprocessing and group-level analysis with a motion covariate. Due to the large number of FDR-corrected significant connections, only connections that surpassed a Bonferroni-corrected statistical threshold (corrected $p<0.05$, uncorrected $p<1.4\times10^{-6}$) are displayed.

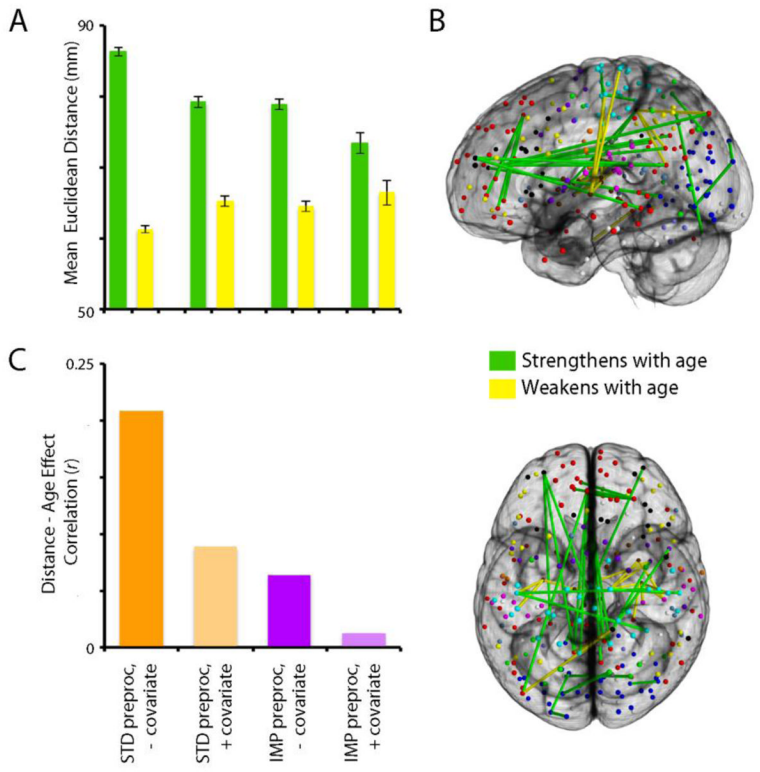

Figure 4.

Motion artifact inflates estimation of distance-dependent change in functional connectivity during adolescence. Both subject- and group-level strategies for controlling the influence of motion artifact reduce the difference in Euclidean distance between connections that strengthen with age and those that weaken with age (**A**). Mean distance in was calculated from connections that were found to be significant above a threshold defined by FDR ($Q<0.05$); error bars represent standard error of the mean. However, even following both improved preprocessing and group-level covariation, connections that strengthen with age were found to be significantly longer than those that weaken with age (**A** & **B**). Due to the large number of connections present, only connections that surpassed a Bonferroni-corrected statistical threshold of $p<0.05$ are displayed. In contrast, when all connections are considered (instead of only connections that significantly change with age), more stringent control of motion artifact abolishes the modulation of age-dependent change in connectivity by distance (**C**). The y-axis represents the correlation between the z-transformed age-connectivity correlation and inter-node Euclidean distance.

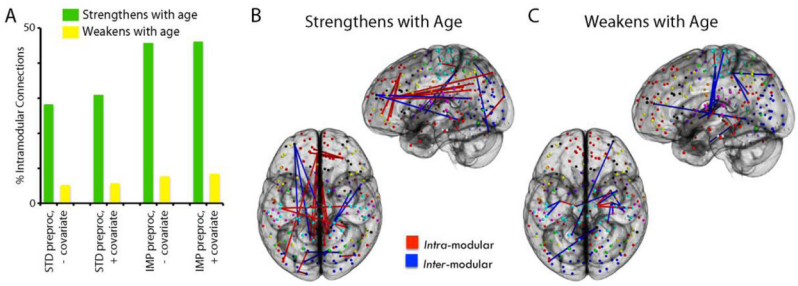

Figure 5.

Accounting for motion allows improved ability to detect development of within-module connections. As previously reported, connections that strengthen with age are more likely to be within-module than between-module. However, improved preprocessing enhances this effect (**A**). Additionally, both subject- and group-level strategies for accounting for motion also result in a greater proportion of within-module age-negative connections, although the overall proportion of these remained quite low. Bar chart represents the percentage of significant (FDR $Q<0.05$) age-positive connections (green) or age-negative connections (yellow) that are intra-modular. Following both improved preprocessing and group-level covariation, the majority of connections that strengthen with age are intra-modular (red connections; **B**), whereas most age-negative connections remained inter-modular (blue connections; **C**). As prior, connections displayed were significant beyond a Bonferroni-corrected threshold of $p<0.05$.

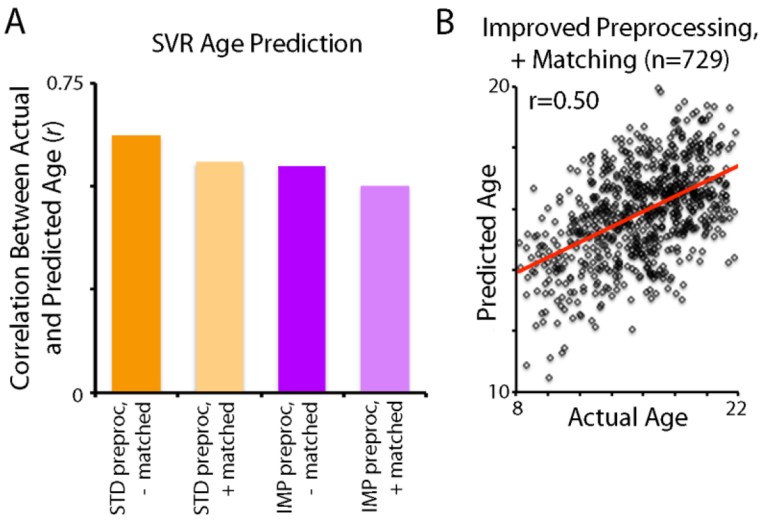

Figure 6.

Correction of motion artifact impacts the accuracy of age prediction using multivariate patterns of functional connectivity, but accuracy nevertheless remains high. Compared to an unmatched sample that that received standard preprocessing, age-motion matching and improved preprocessing reduced the degree to which the complex pattern of functional connectivity could be used to predict subject age using a 10-fold cross-validated linear support vector regression (SVR; **A**). However, the predictive ability of the model even after accounting for motion remained high (r=0.5, permutation-based p<0.001; **B**).

Table 1

Subject demographics in complete sample and sub-samples.

Sample	n	Age (y)	# Males	MRD (mm)	Age-MRD Correlation (r value)
Complete sample	780	15.63 (3.29)	333	0.06 (0.03)	−0.19
Age-motion matched	729	15.91 (3.09)	306	0.06 (0.03)	−0.009
Nearly-motionless	70	16.83 (3.00)	31	0.0265 (0.005)	−0.002